Robotica (1999) volume 17, pp. 523–528. Printed in the United Kingdom © 1999 Cambridge University Press

Dynamic modeling and simulation of a flexible robotic manipulator

V.O. Gamarra-Rosado* and E.A.O. Yuhara†

(Received in Final Form: April 6, 1999)

SUMMARY

This work focuses on the dynamic modeling of a flexible robotic manipulator with two flexible links and two revolute joints, which rotates in the horizontal plane. The dynamic equations are derived using the Newton-Euler formulation and the finite element method, based on elementary beam theory. Computer simulation results are presented to illustrate this study. The dynamic model becomes necessary for use in future design and control applications.

KEYWORDS: Advanced manufacturing technologies; Robotics; Flexible robotic manipulator; Dynamic modeling and simulation; Vibration active control.

1. INTRODUCTION

One matter of increasing interest to control engineers are the effects of flexibility in lightweight manipulators, machine tools and space structures, etc. To achieve the high performance requirements such as high-speed operation, increased accuracy in positioning, lower energy consumption, less weight, and safer operation due to reduced inertia flexible manipulators are recommended. However, in modeling and controlling this manipulator the flexibility of its components must be considered.[1–4] The incorporation of the effects of the flexibility in the system model increases its complexity which, in turn, complicates the problem of controller synthesis. That is, due to the flexibility the position controller of the flexible manipulator must be able to control the motion of the rigid-body mode of the arm and to suppress its vibration modes.[5]

The purpose of this work is to obtain a dynamic model for the design and control of a flexible robotic manipulator. The dynamic model will completely describe motions of a manipulator with flexible links, including large motions, small motions, and their interactions. The robotic manipulator is modeled as being composed of two links attached to each other, with the first link attached to a fixed base. Each link is assumed to be symmetrical about its longitudinal axis in the absence of deformation.

The equations of motion are obtained from the Newton-Euler formulation and the finite element method is utilized to discretize the displacements so that the small motion is represented in terms of nodal displacements. A cubic shape function is assumed for a single beam element in this research. The simulation results were obtained using the *Simulink*, extension to *MatLab* software.

* Division of Mechanical Engineering †Division of Electrical Engineering, College of Engineering – UNESP 12500–000 Guaratinguetá – São Paulo (Brazil). E-mail: victor@feg.unesp.br

2. THE MATHEMATICAL MODEL

In this work it is assumed that the manipulator consists of two revolute joints, modeled as a rigid body, and two flexible links as shown in Figure 1. The original lengths of the upper arm and the lower arm are denoted by l^1 and l^2, respectively. The motion of the manipulator is confined to the horizontal (x,y) plane. This seen on the non-deformed configuration in Figure 1, where the upper arm makes an angle ϕ with respect to the x-axis, and the angle between the upper arm and the lower arm is denoted by γ. The deformed configuration of the flexible manipulator defines two new coordinate systems, (x^1,y^1) and (x^2,y^2), such that the x^1-axis and x^2-axis are parallel to the tangents of the upper arm and the lower arm at the origin and at the joint between the two links, respectively. Let the angle between the x^2-axis and the x-direction be denoted by β. The upper arm and the lower arm are modeled by n beam elements and m beam elements, respectively. Thus there are $n+m+1$ nodal points and each

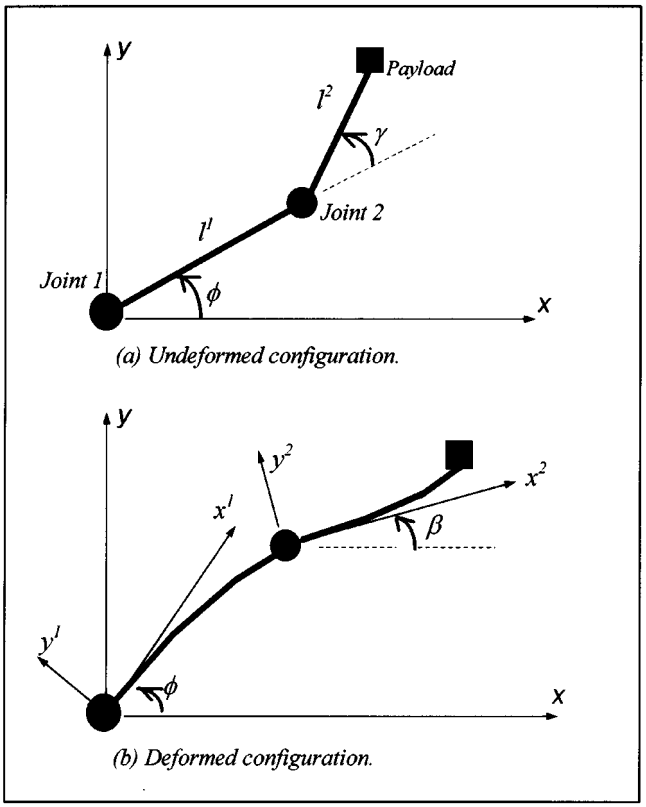


Fig. 1. The configuration of a flexible robotic manipulator.

https://doi.org/10.1017/S0263574799001721 Published online by Cambridge University Press

is associated with a lumped mass. The payloads may also be simulated by the masses attached to some nodal points. The position vector of the generic ith nodal point ($i = 0, 1, 2, \ldots, n$) of the deformed upper arm can be expressed in the (x^1, y^1) coordinate system as

$$\boldsymbol{p}_i^1 \equiv (x_i^1, y_i^1) = \begin{bmatrix} X_i^1 \\ U_i^1 \end{bmatrix} \tag{1}$$

where U_i^1 is the displacement of the ith nodal point in the direction of y^1-axis and the lumped mass at this point is denoted by $\boldsymbol{M}_i^1$. Similarly, the position of the jth nodal point ($j = 0, 1, 2, \ldots, m$) of the deformed lower arm is,

$$\boldsymbol{p}_j^2 \equiv (x_j^2, y_j^2) = \begin{bmatrix} X_j^2 \\ U_j^2 \end{bmatrix} \tag{2}$$

and the lumped mass at this point is denoted by $\boldsymbol{M}_j^2$.

The position vector for any point on the upper arm, expressed in the global coordinate system (x, y), may be obtained as

$$\boldsymbol{p} = \begin{bmatrix} x \\ y \end{bmatrix} = \begin{bmatrix} c\phi & -s\phi \\ s\phi & c\phi \end{bmatrix} \begin{bmatrix} X^1 \\ U^1 \end{bmatrix} \equiv Q^1 \begin{bmatrix} X^1 \\ U^1 \end{bmatrix} \equiv Q^1 \boldsymbol{p}^1 \tag{3}$$

where, Q^1 is an orthogonal transformation matrix, and $c\phi = cos(\phi)$, e $s\phi = sin(\phi)$. The velocity $\boldsymbol{v}$ and the acceleration $\boldsymbol{a}$ can be obtained as,

$$\boldsymbol{v} = \begin{bmatrix} \dot{x} \\ \dot{y} \end{bmatrix} \equiv \begin{bmatrix} -\dot{\phi}s\phi & -\dot{\phi}c\phi \\ \dot{\phi}c\phi & -\dot{\phi}s\phi \end{bmatrix} \begin{bmatrix} X^1 \\ U^1 \end{bmatrix}$$

$$+ Q^1 \begin{bmatrix} 0 \\ \dot{U}^1 \end{bmatrix} \equiv \dot{Q}^1 \boldsymbol{p}^1 + Q^1 \boldsymbol{\nu}^1 \tag{4}$$

$$\boldsymbol{a} \equiv \begin{bmatrix} \ddot{x} \\ \ddot{y} \end{bmatrix} = \begin{bmatrix} -\ddot{\phi}s\phi - \dot{\phi}^2 c\phi & -\ddot{\phi}c\phi + \dot{\phi}^2 s\phi \\ \ddot{\phi}c\phi - \dot{\phi}^2 s\phi & -\ddot{\phi}s\phi - \dot{\phi}^2 c\phi \end{bmatrix} \begin{bmatrix} X^1 \\ U^1 \end{bmatrix}$$

$$+ 2\dot{Q}^1 \boldsymbol{\nu}^1 + Q^1 \begin{bmatrix} 0 \\ \dot{U}^1 \end{bmatrix} \equiv \ddot{Q}^1 \boldsymbol{p}^1 + 2\dot{Q}^1 \boldsymbol{\nu}^1 + \dot{Q}^1 \boldsymbol{a}^1 \tag{5}$$

The position vector of any point on the lower arm, expressed in the global coordinate system (x,y), may be obtained as

$$\boldsymbol{p} = \begin{bmatrix} x \\ y \end{bmatrix} = \begin{bmatrix} c\beta & -s\beta \\ s\beta & c\beta \end{bmatrix} \begin{bmatrix} X^2 \\ U^2 \end{bmatrix}$$

$$+ \begin{bmatrix} c\phi & -s\phi \\ s\phi & c\phi \end{bmatrix} \begin{bmatrix} l^1 \\ U^* \end{bmatrix}$$

$$\equiv Q^2 \boldsymbol{p}^2 + Q^1 \boldsymbol{p}_n^1 \tag{6}$$

where, $U^* \equiv U_n^1$. Then the velocity and the acceleration can be obtained as

$$\boldsymbol{\nu} = \dot{Q}^2 \boldsymbol{p}^2 + Q^2 \boldsymbol{\nu}^2 + \dot{Q}^1 \boldsymbol{p}_n^1 + Q^1 \boldsymbol{\nu}_n^1 \tag{7}$$

$$\boldsymbol{a} = \ddot{Q}^2 \boldsymbol{p}^2 + 2\dot{Q}^2 \boldsymbol{\nu}^2 + Q^2 \boldsymbol{a}^2 + \ddot{Q}^1 \boldsymbol{p}_n^1 + 2\dot{Q}^1 \boldsymbol{\nu}_n^1 + Q^1 \boldsymbol{a}_n^1 \tag{8}$$

where,

$$\boldsymbol{\nu}^2 \equiv \begin{bmatrix} 0 \\ \dot{U}^2 \end{bmatrix}, \quad \boldsymbol{a}^2 \equiv \begin{bmatrix} 0 \\ \ddot{U}^2 \end{bmatrix},$$

$$\boldsymbol{\nu}_n^1 \equiv \begin{bmatrix} 0 \\ \dot{U}^* \end{bmatrix}, \quad \boldsymbol{a}_n^1 \equiv \begin{bmatrix} 0 \\ \ddot{U}^2 \end{bmatrix} \tag{9}$$

The total force acting on a generic point is equal to the inertia force acting on the point, i.e.

$$\boldsymbol{f} = -M\boldsymbol{a} \tag{10}$$

The total force acting on ith nodal point of the upper arm, expressed in the (x^1, y^1) coordinate system, can be calculated as

$$\boldsymbol{f}_i^1 = (Q^1)^T \boldsymbol{f}_i = -M_i^1 (Q^1)^T [\ddot{Q}^1 \boldsymbol{p}^1 + 2\dot{Q}^1 \boldsymbol{\nu}^1 + Q^1 \boldsymbol{a}^1] \tag{11}$$

Explicitly, eq. (11) can be rewritten as

$$f_i^1(x) = M_i^1 [U_i^1 \ddot{\phi} + X_i^1 \dot{\phi}^2 + 2\dot{U}_i^1 \dot{\phi}] \tag{12}$$

$$f_i^1(y) = -M_i^1 [\ddot{U}_i^1 + X_i^1 \ddot{\phi} - U_i^1 \dot{\phi}^2] \tag{13}$$

The total force acting on the jth nodal point of the lower arm can be expressed in the (x^1, y^1) coordinate system and the (x^2, y^2) coordinate system, respectively, as follows

$$\boldsymbol{f}_j^{21} = -M_j^2 (Q^1)^T [\ddot{Q}^2 \boldsymbol{p}^2 + 2\dot{Q}^2 \boldsymbol{\nu}^2 + Q^2 \boldsymbol{a}^2 + \ddot{Q}^1 \boldsymbol{p}_n^1 + 2\dot{Q}^1 \nu_n^1 + Q^1 \boldsymbol{a}_n^1] \tag{14}$$

$$\boldsymbol{f}_j^{22} = -M_j^2 (Q^2)^T [\ddot{Q}^2 \boldsymbol{p}^2 + 2\dot{Q}^2 \boldsymbol{\nu}^2 + Q^2 \boldsymbol{a}^2 + \ddot{Q}^1 \boldsymbol{p}_n^1 + 2\dot{Q}^1 \nu_n^1 + Q^1 \boldsymbol{a}_n^1] \tag{15}$$

Explicitly, eqs. (14–15) can be rewritten as

$$f_j^{21}(x) = +M_j^2 [U^* \ddot{\phi} + l^1 \dot{\phi}^2 + 2\dot{U}^* \dot{\phi} + S\ddot{U}_j^2 + 2C\dot{\beta}\dot{U}_j^2 + (SX_j^2 + CU_j^2)\ddot{\beta} + (CX_j^2 - SU_j^2)\dot{\beta}^2] \tag{16}$$

$$f_j^{21}(y) = -M_j^2 [\ddot{U}^* + l^1 \ddot{\phi} - U^* \dot{\phi}^2 + C\ddot{U}_j^2 - 2S\dot{\beta}\dot{U}_j^2 + (CX_j^2 - SU_j^2)\ddot{\beta} - (SX_j^2 + CU_j^2)\dot{\beta}^2] \tag{17}$$

https://doi.org/10.1017/S0263574799001721 Published online by Cambridge University Press

$$f_j^{22}(x) = +M_j^2[U_j^2\ddot{\beta} + X_j^2\dot{\beta}^2 + 2\dot{U}_j^2\dot{\beta} - S\ddot{U}^* + 2C\dot{U}^*\dot{\phi} - (Sl^1 - CU^*)\ddot{\phi} + (Cl^1 + SU^*)\dot{\phi}^2] \quad (18)$$

$$f_j^{22}(y) = -M_j^2[\ddot{U}_j^2 + X_j^2\ddot{\beta} - U_j^2\dot{\beta}^2 + C\ddot{U}^* + 2S\dot{U}^*\dot{\phi} + (Cl^1 + SU^*)\ddot{\phi} + (Sl^1 - CU^*)\dot{\phi}^2] \quad (19)$$

where, $C \equiv \cos(\beta - \phi)$ and $S \equiv \sin(\beta - \phi)$.

The total force acting on the lower arm is equivalent to a force in the x^1-direction, F_x, a force in the y^1-direction, F_y, and a bending moment T_2, acting at the joint between the upper arm and the lower arm (see Figure 2). These resultant forces and moment may be written as

$$F_x = \sum_{j=1}^{m} f_j^{21}(x) = +\Gamma(U^*\ddot{\phi} + l^1\dot{\phi}^2 + 2\dot{U}^*\dot{\phi}) + \sum_{j=1}^{m} M_j^2[S\ddot{U}_j^2 + (SX_j^2 + CU_j^2)\ddot{\beta} + 2C\dot{\beta}\dot{U}_j^2 + (CX_j^2 - SU_j^2)\dot{\beta}^2] \quad (20)$$

$$F_y = \sum_{j=1}^{m} f_j^{21}(y) = -\Gamma(\ddot{U}^* + l^1\ddot{\phi} - U^*\dot{\phi}^2) - \sum_{j=1}^{m} M_j^2[C\ddot{U}_j^2 + (CX_j^2 - SU_j^2)\ddot{\beta} - 2S\dot{\beta}\dot{U}_j^2 - (SX_j^2 + CU_j^2)\dot{\beta}^2] \quad (21)$$

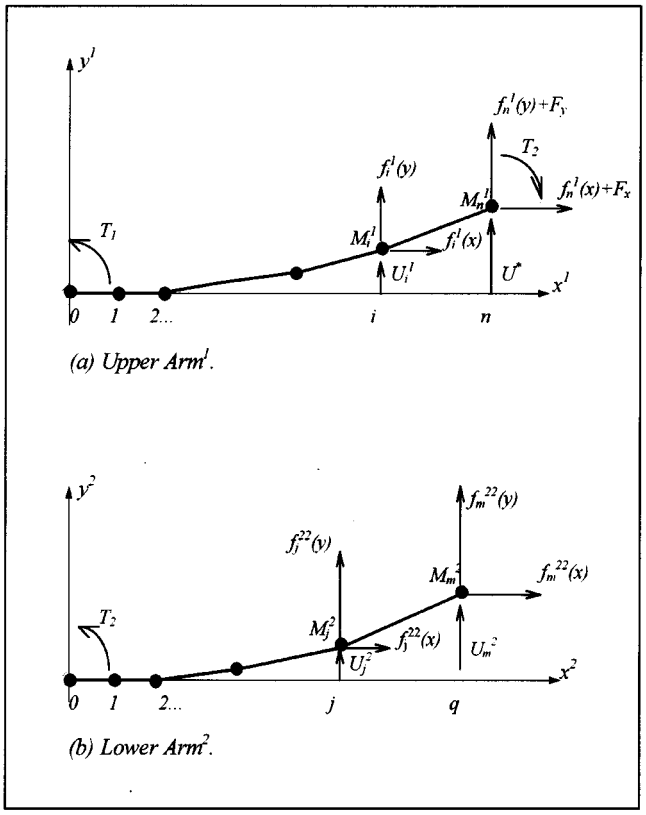


Fig. 2. The forces and moment acting on the two links.

$$T_2 = \sum_{j=1}^{m} [f_j^{22}(x)U_j^2 - f_j^{22}(y)X_j^2] = \sum_{j=1}^{m} M_j^2\{X_j^2\ddot{U}_j^2 + (CX_j^2 - SU_j^2)\ddot{U}^* + (Cl^1X_j^2 + SU^*X_j^2 - Sl^1U_j^2 + CU^*U_j^2)\ddot{\phi} + ((X_j^2)^2 + (U_j^2)^2)\ddot{\beta} + 2\dot{U}^*(SX_j^2 + CU_j^2)\dot{\phi} + (Sl^1X_j^2 - CU^*X_j^2 + Cl^1U_j^2 + SU^*U_j^2)\dot{\phi}^2 + 2U_j^2\dot{U}_j^2\dot{\beta}\} \quad (22)$$

where, $\Gamma = \sum_{j=1}^{m} M_j^2$.

Similarly, the total moment acting on the origin, T_1, can be obtained as

$$T_1 = \sum_{i=1}^{n} [f_i^1(x)U_i^1 - f_i^1(y)X_i^1] + F_y l^1 - F_x U^* + T_2 = +\sum_{i=1}^{n-1} M_i^1 X_i^1 \ddot{U}_i^1 + (M_n^1 + \Gamma)l^1\ddot{U}^* + (Cl^1 + SU^*)\sum_{j=1}^{m} M_j^2\ddot{U}_j^2 + \ddot{\phi}\left[\Gamma((l^1)^2 + (U^*)^2) + \sum_{i=1}^{n} M_i^1((X_i^1)^2 + (U_i^1)^2)\right] + \ddot{\beta}\left\{\sum_{j=1}^{m} M_j^2[(Cl^1 + SU^*)X_j^2 - (Sl^1 - CU^*)U_j^2]\right\} + 2\dot{\phi}(\Gamma U^*\dot{U}^* + \sum_{i=1}^{n} M_i^1 U_i^1 \dot{U}_i^1) - 2\dot{\beta}(Sl^1 - CU^*)\sum_{j=1}^{m} M_j^2\dot{U}_j^2 - \dot{\beta}^2\left\{\sum_{j=1}^{m} M_j^2[(Cl^1 + SU^*)U_j^2 + (Sl^1 - CU^*)X_j^2]\right\} + T_2 \quad (23)$$

3. ANALYSIS BY FINITE ELEMENT METHOD

Now, the two link manipulator can be treated as two cantilever beams on which the forces and moment, are acting, as shown in Figure 2. Following standard procedures in finite element analysis[6] and the elementary beam theory, one may obtain the governing equations for the lower arm (beam 2), as follows[7]

$$\boldsymbol{K^2U^2 = f^{22}} \quad (24)$$

https://doi.org/10.1017/S0263574799001721 Published online by Cambridge University Press

where

$$\boldsymbol{U}^2 \equiv (U_1^2, U_2^2, U_3^2, \ldots, U_m^2)^T \tag{25}$$

$$\boldsymbol{f}^{22} \equiv [f_1^{22}(y), f_2^{22}(y), f_3^{22}(y), \ldots, f_m^{22}(y)]^T \tag{26}$$

and $\boldsymbol{K}^2$ is the $(m \times m)$ stiffness matrix for a cantilever beam subjected to applied forces only. For the upper arm (beam 1), because there is a bending moment, T_2, acting at the free end of beam 1 (see Figure 2), following the same procedure outlined in reference 7, the governing equations may be written as

$$\begin{bmatrix} \boldsymbol{K}' & \boldsymbol{K} \\ \boldsymbol{K}^T & k \end{bmatrix} \begin{bmatrix} \boldsymbol{U}^1 \\ s \end{bmatrix} = \begin{bmatrix} \boldsymbol{f}' \\ T_2 \end{bmatrix} \tag{27}$$

where

$$\boldsymbol{U}^1 \equiv (U_1^1, U_2^1, U_3^1, \ldots, U_n^1)^T \tag{28}$$

$$\boldsymbol{f}' \equiv (f_1^1(y), f_2^1(y), f_3^1(y), \ldots, f_n^1(y) + F_y) \tag{29}$$

and s is the slope at the free end of beam 1; $\boldsymbol{K}'$ is a $(n \times n)$ matrix; $\boldsymbol{K}$ is a vector of length n and it can be written as $(K_1, K_2, \ldots, K_n)^T$. By eliminating s from equation (27), the following is obtained

$$\boldsymbol{K}^1 \boldsymbol{U}^1 = \boldsymbol{f}' - \frac{\boldsymbol{K} T_2}{k} \tag{30}$$

and, $\boldsymbol{K}^1 = \boldsymbol{K}' - \dfrac{\boldsymbol{K}\boldsymbol{K}^T}{k}$.

Now equations (24), (30), (22) and (23) may be rewritten in a more compact form as follows

$$\begin{bmatrix} \boldsymbol{a}_1 & 0 & \boldsymbol{b} \\ 0 & \boldsymbol{a}_2 & \boldsymbol{c} \\ \boldsymbol{b}^T & \boldsymbol{c}^T & \boldsymbol{a}_3 \end{bmatrix} \ddot{\omega} \equiv \Omega \tag{31}$$

where

$$\omega \equiv (U_1^1, U_2^1, \ldots, U_{n-1}^1, U_1^2, U_2^2, \ldots, U_m^2, U_n^1, \beta, \phi)^T \tag{32}$$

$$\boldsymbol{a}_1 \equiv \begin{bmatrix} M_1^1 & 0 & \ldots & 0 \\ 0 & M_2^1 & \ldots & 0 \\ \vdots & & & \\ 0 & 0 & \ldots & M_{n-1}^1 \end{bmatrix} \tag{33}$$

$$\boldsymbol{a}_2 \equiv \begin{bmatrix} M_1^2 & 0 & \ldots & 0 \\ 0 & M_2^2 & \ldots & 0 \\ \vdots & & & \\ 0 & 0 & \ldots & M_m^2 \end{bmatrix} \tag{34}$$

$$\boldsymbol{a}_3 \equiv \begin{bmatrix} A_1 & A_4 & l^1 A_1 \\ A_4 & A_2 & A_5 \\ l^1 A_1 & A_5 & A_3 \end{bmatrix} \tag{35}$$

$$\boldsymbol{b} \equiv \begin{bmatrix} 0 & 0 & M_1^1 X_1^1 \\ 0 & 0 & M_2^1 X_2^1 \\ \vdots & \vdots & \vdots \\ 0 & 0 & M_{n-1}^1 X_{n-1}^1 \end{bmatrix} \tag{36}$$

$$\boldsymbol{c} \equiv \begin{bmatrix} C_{11} & C_{21} & C_{31} \\ C_{12} & C_{22} & C_{32} \\ \vdots & \vdots & \vdots \\ C_{1m} & C_{2m} & C_{3m} \end{bmatrix} \tag{37}$$

$$\Omega \equiv (p_1, p_2, \ldots, p_{n-1}, q_1, q_2, \ldots, q_m, \gamma_1, \gamma_2, \gamma_3)^T \tag{38}$$

$$A_1 \equiv M_n^1 + \Gamma \tag{39}$$

$$A_2 \equiv \sum_{j=1}^{m} M_j^2 [(X_j^2)^2 + (U_j^2)^2] \tag{40}$$

$$A_3 \equiv \sum_{i=1}^{n} M_i^1 [(X_i^1)^2 + (U_i^1)^2] + \Gamma[(l^1)^2 + (U_n^1)^2] \tag{41}$$

$$A_4 \equiv C \sum_{j=1}^{m} M_j^2 X_j^2 - S \sum_{j=1}^{m} M_j^2 U_j^2 \tag{42}$$

$$A_5 \equiv (Cl^1 + SU^*) \sum_{j=1}^{m} M_j^2 X_j^2 - (Sl^1 - CU^*) \sum_{j=1}^{m} M_j^2 U_j^2 \tag{43}$$

$$c_{1j} \equiv CM_j^2, \quad c_{2j} \equiv M_j^2 X_j^2, \quad c_{3j} \equiv M_j^2 (Cl_1 + SU^*) \tag{44}$$

$$p_i \equiv -\sum_{j=1}^{n} K_{ij}^1 U_j^1 + M_i^1 U_i^1 \dot{\phi}^2 - \left(\frac{K_i}{k}\right) T_2 \tag{45}$$

$$q_i \equiv -\sum_{j=1}^{m} K_{ij}^2 U_j^2 - 2S\dot{U}^* \dot{\phi} M_i^2 + \dot{\beta}^2 U_i^2 M_i^2 - (Sl^1 - CU^*)\dot{\phi}^2 M_i^2 \tag{46}$$

$$\gamma_1 \equiv -\sum_{j=1}^{n} K_{nj}^1 U_j^1 + (M_n^1 + \Gamma) U^* \dot{\phi}^2 - \left(\frac{K_n}{k}\right) T_2 + 2S\dot{\beta} \sum_{j=1}^{m} M_j^2 \dot{U}_j^2 + \dot{\beta}^2 \sum_{j=1}^{m} (SX_j^2 + CU_j^2) M_j^2 \tag{47}$$

$$\gamma_2 \equiv T_2 - 2\dot{U}^* \dot{\phi} \sum_{j=1}^{m} M_j^2 (SX_j^2 + CU_j^2) - 2\dot{\beta} \sum_{j=1}^{m} M_j^2 U_j^2 \dot{U}_j^2 - \dot{\phi}^2 \sum_{j=1}^{m} M_j^2 (Sl^1 X_j^2 - CU^* X_j^2 + Cl^1 U_j^2 + SU^* U_j^2) \tag{48}$$

https://doi.org/10.1017/S0263574799001721 Published online by Cambridge University Press

Table I. Manipulator model parameters.

Length of link 1 and 2	0.3 m
Cross-section area of links	0.127×10^{-4} m^2
Cross-section area moment of inertia about z-axis	0.3×10^{-12} m^4
Young's modulus of elasticity	1.3×10^{12} N/m^2
Mass per unit length	0.1 kg/m
Joint 1 and 2 masses	8×10^{-2} kg
Nominal payload	2×10^{-3} kg
Number of beam elements	4

$$\gamma_3 \equiv T_1 - T_2 - 2\dot{\phi}\left(\Gamma U^* \dot{U}^* + \sum_{i=1}^{n} M_i^1 U_i^1 \dot{U}_1^1\right)$$

$$+ 2\dot{\beta}(Sl^1 - CU^*)\sum_{j=1}^{m} M_j^2 \dot{U}_j^2$$

$$+ \dot{\beta}^2\left\{\sum_{j=1}^{m} M_j^2\,[(Cl^1 + SU^*)U_j^2 + (Sl^1 - CU^*)X^2]\right\} \quad (49)$$

4. SIMULATION RESULTS

To illustrate the effects of the flexibility in the robotic manipulator the parameters of Table I are used. The simulation was done to maneuver the arm from $\phi_i = 0$ [rad] to $\phi_f = 0.768$ [rad] and $\beta_i = 0$ [rad] to $\beta_f = 0.384$ [rad], during 1.5 seconds. Figures 3 and 4 show that the system response is obtained with a simple joint control PD; this illustrates the importance of the flexibility effects.

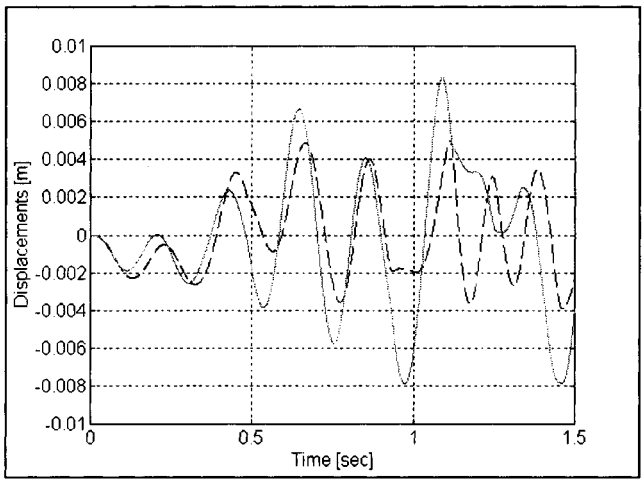


Fig. 3. Flexible manipulator model simulation: Tip vibrations.

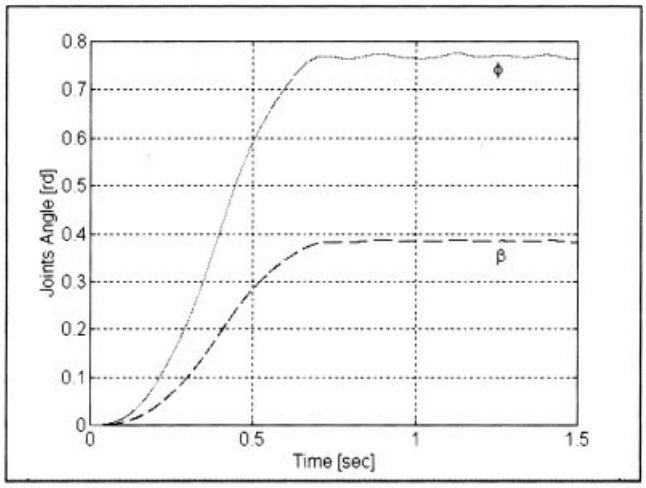


Fig. 4. Flexible manipulator model simulation: Joint angles.

Figure 3 shows the response of the end-point of the flexible manipulator (dashed plot) and the displacements of the free end of the link 1 (joint 2). Figure 4 shows the effects of these displacements in the joints during the maneuver.

5. CONCLUSION

In this work, we obtained a dynamic model of a planar flexible robotic manipulator which has two revolute joints and two flexible links. The governing equations of the system are nonlinear. Axial deformations are neglected and only the transverse bending displacements are dominant in the theoretical modeling of this manipulator. Viscous damping at the joints is ignored.

The flexibility of the system degrades the function of the position controller of the end-effector; thus, it must be taken into account, since flexibility limits the system stability, the accuracy of operations and control gains. Here the flexible manipulator is under a co-located PD output feedback control using hub angle measurements. The PD controller parameters are adjusted relative to the arm flexibility to illustrate the effects of flexibility.

For digital control systems, flexibility will also affect the sampling rate. However, one may have to construct an estimator (observer) based on the linear version of the system which involves few variables. Hence, for practical purposes, real-time control of flexible robotic manipulator is feasible.

References

1. W.J. Book, "Recursive Lagrangian dynamics of flexible manipulator arms" *Int. J. Rob. Res.* **3**, No. 3, 87–101 (1984).
2. W.H. Sunada and S. Dubowsky, "On the dynamic analysis and behavior of industrial robotic manipulators with elastic members" *Transactions of the ASME Journal of Mechanisms, Transmission and Automation in Design* **105**, No. 1, 42–51 (1983).
3. L.W. Chang and J.F. Hamilton, "Dynamics robotic manipulators with flexible links" *Transactions of the ASME Journal of Dynamic Systems, Measurement, and Control* **113**, No. 1, 54–59 (1991).

https://doi.org/10.1017/S0263574799001721 Published online by Cambridge University Press

4. V.O. Gamarra-Rosado and D.E. Zampieri, "Experimental dynamic validation of a flexible one-link arm" in J.M. Balthazar, D.T. Mook and J.M. Rosário, Eds, *Nonlinear Dynamics, Chaos, Control, and Their Applications to Engineering Sciences,* **Vol. 1** (1997), pp. 326–330.
5. V.O. Gamarra-Rosado, G. Fernández, J.C. Grieco, M. Armada and N. Aliane, "Automation and Cybernetics: Control of a flexible one-link manipulator" *Kybernetes* **25**, No. 5, 38–47 (1996).
6. J.S. Przemieniecki, *Theory of Matrix Structural Analysis* (McGraw-Hill, New York, 1986).
7. J.D. Lee, L.S. Haynes, B.L. Wang and K.-H. Tsai, "Control of flexible robot arm" *Proceedings of the ASME Winter Annual Meeting*, Boston (1987), pp. 241–251.

https://doi.org/10.1017/S0263574799001721 Published online by Cambridge University Press